Oxidative decomposition of butyl acetate by micro-nano bubbles at room temperature

Juan Hu[a], **Ya-zhuo Hao**[a], **Jian-jun Wei**[a,b,*], **Zhong-ming Guo**[a], **William Bai**[a]

[a] Institute of Atomic and Molecular Physics, Sichuan University, Chengdu 610065 China
[b] Sichuan Profit Energy Technology Co. Ltd., Chengdu 610047 China

*Corresponding author, e-mail: weijianjun@scu.edu.cn

ABSTRACT: In this work, the degradation of low-concentration butyl acetate was performed in a micro-nano bubble device via the cavitation effect. The degradation efficiency of this process was investigated for different butyl acetate concentrations. The experimental results showed that with a butyl acetate concentration of 186.5 mg/m^3, the degradation efficiency of butyl acetate was 77.6%. Gas chromatography-mass spectrometry was used to identify the intermediate products generated during different treatment periods under varying initial concentrations. Based on the product analysis, the degradation reaction and pathway were speculated. All the results showed that the major reaction pathway of butyl acetate degradation was the initial production of low-carbon ester, which was then decomposed into butyl alcohol and acetone compounds. This study provides a deeper understanding of the degradation of butyl acetate by micro-nano bubbles and the mechanism of degradation.

KEYWORDS: micro-nano bubbles, cavitation, butyl acetate

INTRODUCTION

Volatile organic compounds (VOCs) are the primary precursor of PM2.5 and O$_3$ [1]. Among them, butyl acetate has a significant impact on air pollution [2]. Butyl acetate is widely derived from coatings [3], chemicals [4], packaging, and printing materials [5]. Therefore, one of the focal issues of air pollution control is the degradation of ester waste gas [6]. There are many methods for degrading VOCs, including adsorption [7], catalytic oxidation [8], and plasma system decomposition [9]. Keller et al [10] reported the treatment of butyl acetate via photocatalysis using TiO$_2$, Pt/TiO$_2$, and WO$_3$/TiO$_2$ semiconductor catalysts. However, photocatalyst deactivation was a problem that requires further investigation, and the light utilization efficiency of these catalysts was also very low. Mull et al [11] investigated the photocatalytic degradation of butyl acetate under UV and blue LED light in 1 m^3 (40% relative humidity) and 20 l (0% relative humidity) emission test chambers with TiO$_2$-GO composite catalysts. However, their proposed method only partially degraded butyl acetate, with a low degradation efficiency range of 10–39% under blue light [11]. Absorption methods have also been extensively studied for the abatement of butyl acetate. Wang et al [12] described the use of a 1:1 mixture of methyl oleic acid and ethyl oleic acid as a butyl acetate absorbent. However, absorbents need to be regularly replaced, so the material cost of adsorption methods is high. Moreover, butyl acetate degradation methods still exhibit many deficiencies, such as safety risks [13], high costs [14], and the generation of secondary pollution [15]. With increasingly strict en-

vironmental regulations around the world, the market demand for environmental protection technology and equipment is growing. Absorption and photocatalytic degradation methods do not meet the realistic needs and achieve the standard of direct emission. Hence, the development of innovative treatment technology is required to meet modern environmental rules.

Due to their large specific surface area, high mass transfer efficiency and long residence time, micro-nano bubbles were widely used for the treatment of organics such as rhodamine B [16] and alachlor [17]. Liu [8] used micro-nano bubbles for the treatment of ink wastewater. They reported that organic matter was removed five times more rapidly using micro-nano bubbles compared with ordinary dissolved air bubbles. Micro-nano bubbles can generate free radicals, which decompose large molecules into smaller molecules. Moreover, micro-nano bubbles can synergistically interact with ozone and hydrogen peroxide to improve degradation performance. Xia et al [19] achieved the efficient degradation of methyl orange wastewater by combining micro-nano bubbles with ozone. Many other micro-nano bubble applications have also been reported [20]. However, to the best of our knowledge, only a few studies exist on the degradation of acetate exhaust using micro-nano bubbles.

In this study, the degradation of butyl acetate was investigated using micro-nano bubble technology. To demonstrate the degradation effect of the micro-nano bubbles, this study was carried out using low concentrations of butyl acetate gas molecules. The reaction principle and the butyl acetate route in the micro-nano bubble device were established by tracking the intermediate products. This study provides a new
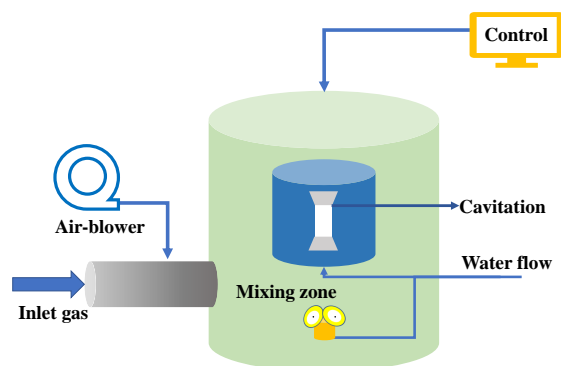
Fig. 1 Schematic diagram of the experimental micro-nano bubble device.

method for degrading VOCs using water as a medium at ambient temperature and pressure.

MATERIALS AND METHODS

Experimental apparatus

Experimental tests were carried out in a micro-nano bubble device located at Sichuan University. This device was a closed circulation system consisting of a master control system, a micro-nano bubble system, a water circulation system, and a cyclone system, as shown in Fig. 1. The micro-nano bubble system consisted of a nozzle and a crushing device. The interior design of the nozzle was similar to a venturi, and many hard and sharp crushing needles were placed on the crushing device. The local pressure in this system fell to the value of the vapor pressure of the liquid medium as the fluid passed through the throat of the micro-nano bubbles system [21]. This droves the growth of micro-nano cavitation nuclei in the liquid [22]. When the growing bubbles reached the high-pressure area with the fluid, the collapse of these bubbles led to localized high-temperature and high-pressure conditions, which degraded the exhaust gas [23]. The spray was installed at the bottom of the micro-nano bubble system to trap the gas and enhance the mass transfer efficiency of the bubbles in the water.

Degradation experiments

A vessel containing butyl acetate was placed to simulate industrial exhaust gas. Butyl acetate (99.5%, AR grade) was purchased from Chengdu Kelong Chemical Co., Ltd. The butyl acetate concentrations in the micro-nano bubble device were monitored using a PID (Mini-RAE 3000). Butyl acetate was swept by the air-blower for five seconds to generate a homogeneous gas. The stability values of the experiment were recorded. After each experiment, samples were collected using a 20 ml sample bottle or a Teflon gas bag. The intermediate products of the butyl acetate degradation process were

analyzed by gas chromatography-mass spectrometry (GC-MS). This experiment used a QP2010 Plus temperament joint instrument (SHIMADZU, Japan). Samples were injected in split mode and the inlet temperature was 270 °C. The column flow rate was 1 ml/min, and the volume of injected sample was 1 ml. The MS (EI-source at 200 °C) was operated in scan mode (m/z 30–500 amu) with a solvent delay at 0.1 min.

RESULTS AND DISCUSSION

Feasibility analysis of micro-nano bubble system

To determine the degradation effect of the micro-nano bubble process on VOCs, preliminary experiments were performed with varying butyl acetate concentrations (186.5 mg/m^3, 245.6 mg/m^3, and 313.9 mg/m^3), as shown in Fig. 2(a). These experiments showed that the initial concentration of butyl acetate was reduced with increasing treatment time. Under each initial butyl acetate concentration, the total concentration sharply decreased at $t = 10$ min. The total concentration of butyl acetate dropped to 112.7 mg/m^3 from the initial 313.9 mg/m^3. The three experiments displayed similar degradation trends, and the degradation effect was relatively stable within the tested concentration range. However, when the initial concentration was increased, fewer micro-nano bubbles in the cavitation zone were accessible per butyl acetate molecule [24]. Therefore, the range of action and the transmitted energy of these micro-nano bubbles were not sufficient to completely degrade all the butyl acetate molecules [25]. Consequently, the concentrations of butyl acetate after the degradation process in the micro-nano bubble device were maintained in a certain range. The butyl acetate degradation efficiency of this system was calculated as follows:

$$\eta = \frac{C_0 - C_n}{C_0} \times 100\%$$

where η is the degradation efficiency and C_0 and C_n are the inlet and outlet concentrations of butyl acetate, respectively.

Fig. 2(b) shows the butyl acetate degradation efficiencies for the different initial concentrations. For the initial butyl acetate concentrations of 186.5 mg/m^3, 245.6 mg/m^3, and 313.9 mg/m^3, butyl acetate degradation efficiencies of 65.7–77.6%, 52.6–61.5%, and 53.8–64.1% were achieved, respectively. These results showed that the maximum degradation effect was achieved at 30 min and the micro-nano bubble device was highly efficient for butyl acetate concentrations below 200 mg/m^3. However, the treatment efficiency was not sensitive for concentrations that exceeded this limit. This was potentially attributed to the limitations of the existing conditions. This processing limitation was difficult to overcome. Therefore, changing the structure of the micro-nano bubble device or increasing the number of reactors would be required to improve
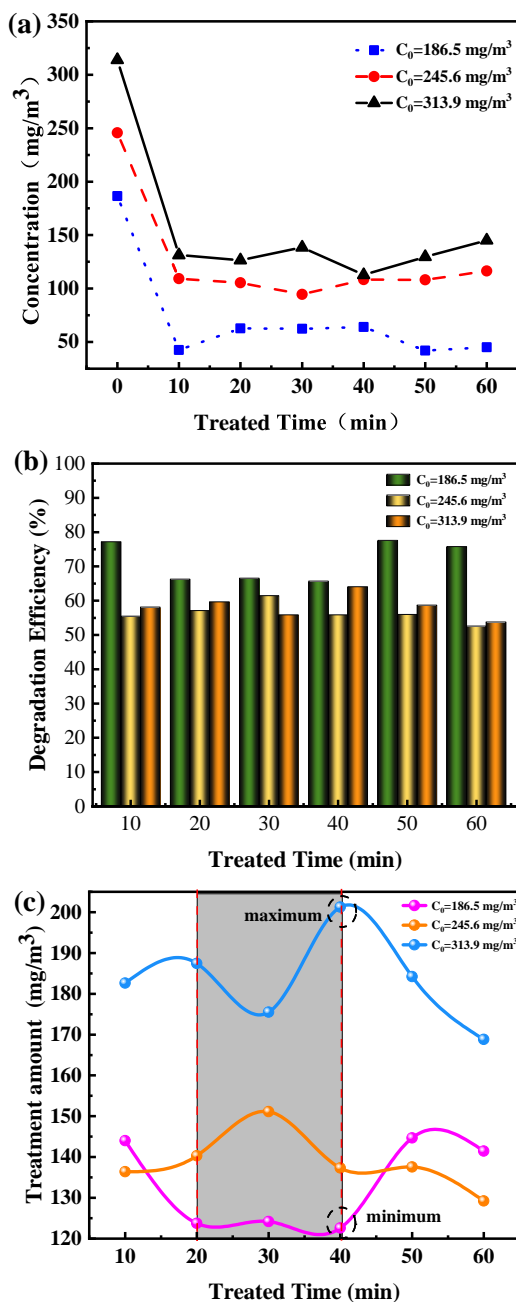
Fig. 2 Effect of the initial butyl acetate gas concentration on (a) post-degradation butyl acetate concentration, (b) degradation efficiency, and (c) amount of treated butyl acetate.
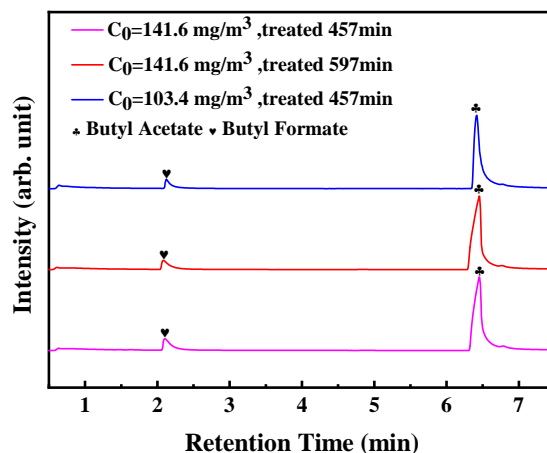

Fig. 3 Total ion chromatograms obtained by GC-MS analysis of water samples taken from the micro-nano bubble device after butyl acetate degradation.
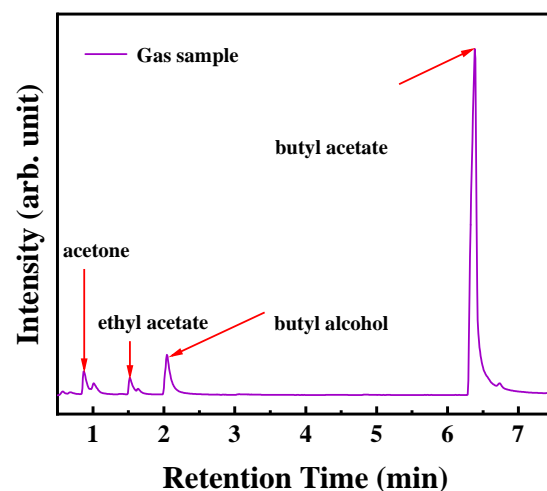

Fig. 4 Total ion chromatogram obtained by GC-MS analysis of the gas sample using an inlet butyl acetate concentration of 107.8 mg/m^3 and a treatment time of 547 min.

the degradation efficiency. Interestingly, Fig. 2(c) shows that despite the low degradation efficiency for initial concentrations above 200 mg/m^3, the amount of treated butyl acetate increased with increasing initial concentration. When the initial butyl acetate concentration was increased from 186.5 mg/m^3 to 313.9 mg/m^3, the amount of treated butyl acetate

increased from 122.6 mg/m^3 to 201.3 mg/m^3. This was likely because the probability of collisions between butyl acetate and micro-nano bubbles increased with increasing initial concentration.

Degradation products

To identify the reaction products, additional experiments were conducted at initial butyl acetate concentrations of 103.4 mg/m^3 and 141.6 mg/m^3 in 20 °C water. The butyl acetate degradation efficiencies achieved with these initial concentrations were 64% and 64.4%, respectively. Total ion chromatographs of the post-reaction water obtained from the micro-nano bubble

Table 1 Degradation products obtained after the degradation of butyl acetate.

Name	Formula	MW	RI	RT (min)	Peak Area (%)
Acetone	C_3H_6O	58	455	0.872	1.58
Butyl Alcohol	C_4H_{10}	74	662	2.044	2.74
Ethyl Acetate	$C_4H_8O_2$	88	586	1.520	1.14
Butyl Formate	$C_5H_{10}O_2$	102	783	2.08;2.103;2.125	10.4;12.98;9.09
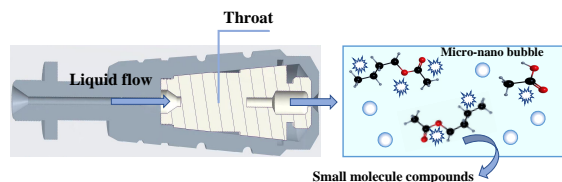
Fig. 5 Schematic diagram of the micro-nano bubble reactor and the butyl acetate degradation process.

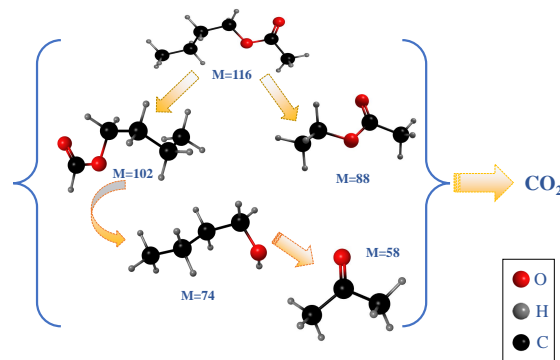**Fig. 6** Possible reaction pathway for the degradation of butyl acetate.

device are shown in Fig. 3. For the experiment with an initial butyl acetate concentration of 141.6 mg/m^3, the butyl acetate peak area was reduced to 88.6% and 85.88% after 457 min and 597 min treatment, respectively. This indicated that the butyl acetate content gradually decreased after 140 min treatment.

For the experiment with an initial butyl acetate concentration of 141.6 mg/m^3, the main characteristic peak of the generated butyl formate was observed, with an increase in peak area from 10.4% to 12.98% after 457 min and 597 min treatment. This result implied that butyl acetate was degraded to form butyl formate. At the same treatment time, the butyl formate yield was 9.09% for an initial butyl acetate concentration of 103.4 mg/m^3. This was lower than the butyl formate yield of the experiment with an initial butyl acetate concentration of 141.6 mg/m^3. This was consistent with the results reported in the previous section, in which a lower initial butyl acetate concentration led to lower amount of treated butyl acetate and therefore a lower yield of intermediate products.

Fig. 4 shows that several peaks appeared in the exit gas total ion chromatogram before the butyl acetate peak (retention time $t = 6.383$ min). This indicated that several degradation products were produced during the reaction. A spectrum search of the gas-phase degradation products indicated the presence of butanol, ethyl acetate, and acetone, as shown in Table 1.

Degradation mechanism

Micro-nano bubble technology uses cavitation to create micro-nano bubbles. When these bubbles are ruptured, they generate localized high-temperature and high-pressure conditions, which can crack large molecules into smaller molecules. Researchers have observed micro and nano bubbles through dynamic light scattering in the early [26]. In our experiments,
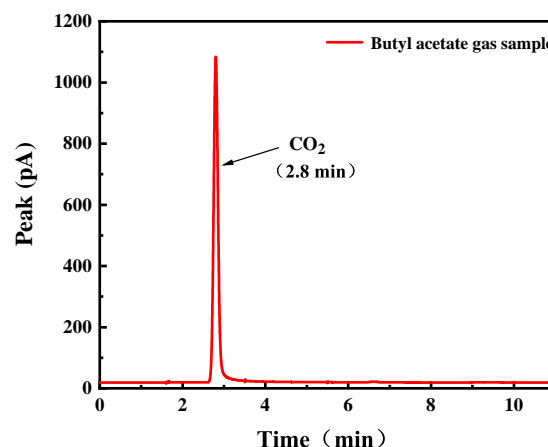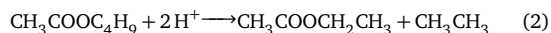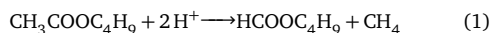

Fig. 7 Chromatogram obtained by GC analysis of the gas phase products after the degradation of butyl acetate using an inlet concentration of 199.2 mg/m^3 and a treatment time of 480 min.

micro-nano bubbles were randomly contracted under the pressure change of the flowing liquid [27, 28]. Subsequently, these bubbles were dispersed by the crushing needle action to produce even smaller bubbles. The micro-nano bubble reactor structure and butyl acetate degradation mechanism are shown in Fig. 5. According to the Young-Laplace equation, the pressure inside a bubble is proportional to its surface tension and inversely proportional to its particle size [29]. The small size of the micro-nano bubbles

leads to very high internal pressure and high energy density. External work is briefly performed when these bubbles collapse. The temperature inside the bubbles sharply increases due to adiabatic compression [30]. Mechanical energy is converted to thermal energy by the law of conservation of energy.

Butyl acetate is insoluble in water. Therefore, butyl acetate degradation reaction primarily occurs at gas-liquid interfaces. The four identified butyl acetate degradation intermediates discussed above were used to propose a potential butyl acetate degradation pathway: First, butyl acetate is adsorbed by the micro-nano bubbles, and the energy generated by the collapse of these micro-nano bubbles directly degrades the butyl acetate molecules into butyl formate and ethyl acetate. Next, these intermediates are further degraded to produce butyl alcohol and acetone. Finally, these intermediate products are degraded to CO_2. A plausible pathway for the cracking of butyl acetate by micro-nano bubbles at low temperatures is proposed in Fig. 6.

The bond dissociation energies of butyl acetate are 3.44 eV for C—C, 3.38 eV for C—O, 4.29 eV for C—H, and 7.55 eV for C=O [31]. According to ionization energies and organic species detected by GC-MS, it was speculated that the butyl acetate degradation mechanism of the micro-nano bubble device potentially favored C—C and C—O bond breakage. These reactions are described as follows:

$$CH_3COOC_4H_9 + 2H^+ \longrightarrow HCOOC_4H_9 + CH_4 \qquad (1)$$

$$CH_3COOC_4H_9 + 2H^+ \longrightarrow CH_3COOCH_2CH_3 + CH_3CH_3 \qquad (2)$$

The degradation of butyl acetate is a process involving coexisting multi-reaction interactions. Butyl formate and ethyl acetate were formed by breaking the C—C bond of butyl acetate, as shown in Eqs. (1) and (2), respectively. This was confirmed by GC-MS.

It has been reported that extreme reaction fields are formed when these bubbles collapse inward [32]. The high temperatures and pressures generated by micro-nano bubble collapse can dissociate water molecules into hydroxyl radicals and hydrogen ions [33]. The organic species that are generated by the cracking of butyl acetate (such as C_2, C_3, and C_4) can react with H and OH. Butyl alcohol was detected by GC-MS, and this compound was potentially derived from the reaction of $CH_3CH_2CH_2CH_2O\cdot$ and H^+, as shown in Eq. (3).

$$HCOOC_4H_9 + H_2O \longrightarrow CH_3CH_2CH_2CH_2OH + HCOOH \qquad (3)$$
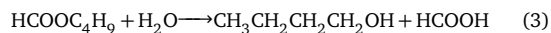
As micro-nano bubbles shrink, excess anions accumulate at the gas-liquid interface, causing a local acid-base imbalance [34]. Therefore, butanol was formed by the hydrolysis of butyl formate and butyl acetate. Upon reaching a critical pressure, micro-nano bubbles will collapse. This sudden change in the gas-liquid interface leads to a sudden release of energy. Under these non-equilibrium conditions, butanol was decomposed. The Gibbs free energy for the hydrolysis of

butyl formate to butanol is -89159.83 kJ/mol, which shows that this reaction is spontaneous. Moreover, the conductivity of the aqueous solution after butyl acetate degradation was measured. Based on its conductivity, the reaction rate of this reaction is up to 8.93×10^4 l/(mol·min).

The butyl acetate degradation products mainly included esters, alcohols, and acetone. Raillard et al [35] previously reported that acetone can be degraded to formaldehyde, formic acid, or methanol. Eventually, these compounds are degraded into CO_2 and H_2O. In this work, CO_2 was not detected by GC-MS. However, acetone, which has the potential to degrade to CO_2, was detected as an intermediate. The gas product was passed through clarified lime water, which became turbid. This proved that the degradation products were deeply degraded to CO_2. Finally, to quantitatively prove the presence of CO_2, CO_2 was detected by gas chromatography at a detection time of $t = 2.8$ min, as shown in Fig. 7.

CONCLUSION

The degradation of butyl acetate by micro-nano bubble technology was explored. The butyl acetate degradation efficiency was 77.6% for an initial butyl acetate concentration of 186.5 mg/m^3. GC-MS was used to confirm that the intermediates formed in the liquid phase were mainly butyl formate, and the intermediates in the gas phase were mainly butanol, ethyl acetate, and acetone. Moreover, GC analysis demonstrated the generation of CO_2 during the reaction. Based on the identified intermediates, a possible degradation pathway for butyl acetate was proposed. These results demonstrate that micro-nano bubble technology can realize the room-temperature cracking of butyl acetate, which eventually degrade to CO_2.

REFERENCES

1. Zhao YF, Gao J, Cai YJ, Wang JJ, Pan J (2021) Real-time tracing VOCs, O_3 and PM2.5 emission sources with vehicle-mounted proton transfer reaction mass spectrometry combined differential absorption lidar. *Atmos Pollut Res* **12**, 146–153.
2. Cheng Q, Zhang GK (2020) Enhanced photocatalytic performance of tungsten-based photocatalysts for degradation of volatile organic compounds: a review. *Tungsten* **2**, 240–250.
3. Wong CT, Abdullah AZ, Bhatia S (2008) Catalytic oxidation of butyl acetate over silver-loaded zeolites. *J Hazard Mater* **157**, 480–489.
4. Liu RJ, Wei KN, Zhao H, Jin YM, Zhang ZC (2013) Recovery of butyl acetate from wastewater by ionic liquid extraction. *Environ Prot Chem Ind* **33**, 108–110.
5. Wang JD, Lu JZ, Li WJ, Gu ZY, Miao XP (2018) Pollution characteristics and emission coefficients of volatile organic compounds from the packaging and printing industry in Zhejiang Province. *Environ Sci* **39**, 3552–3556.
6. Lovascio S, Blin-Simiand N, Magne L, Jorand F, Pasquiers S (2014) Experimental study and kinetic modeling for

ethanol treatment by air dielectric barrier discharges. *Plasma Chem Plasma Process* **35**, 279–301.

7. Ma XL, Wang WL, Sun CG, Li H, Sun J, Liu X (2021) Adsorption performance and kinetic study of hierarchical porous Fe-based MOFs for toluene removal. *Sci Total Environ* **793**, 148622.

8. Liu RY, Zhou B, Liu LZ, Zhang Y, Chen Y, Zhang QL, Yang ML, Hu LP, et al (2021) Enhanced catalytic oxidation of VOCs over porous Mn-based mullite synthesized by *in-situ* dismutation. *J Colloid Interface Sci* **585**, 302–311.

9. Cai SC, Li JJ, Yu EQ, Chen X, Chen J, Jia HP (2018) Strong photothermal effect of plasmonic Pt nanoparticles for efficient degradation of volatile organic compounds under solar light irradiation. *ACS Appl Nano Mater* **1**, 6368–6377.

10. Keller V, Bernhardt P, Garin F (2003) Photocatalytic oxidation of butyl acetate in vapor phase on TiO_2, Pt/TiO_2 and WO_3/TiO_2 catalysts. *J Catal* **215**, 129–138.

11. Mull B, Möhlmann L, Wilke O (2017) Photocatalytic degradation of toluene, butyl acetate and limonene under UV and visible light with titanium dioxide-graphene oxide as photocatalyst. *Environments* **4**, 9.

12. Wang J, Yuan D, Deng Y, Wu L, Lu J, Yang Z (2019) Study on treatment process of butyl acetate waste gas. *Appl Chem Ind* **48**, 830–833.

13. Kamal MS, Razzak SA, Hossain MM (2016) Catalytic oxidation of volatile organic compounds (VOCs): a review. *Atmos Environ* **140**, 117–134.

14. Kasperczyk D, Urbaniec K, Barbusinski K, Rene ER, Colmenares-Quintero RF (2019) Application of a compact trickle-bed bioreactor for the removal of odor and volatile organic compounds emitted from a wastewater treatment plant. *J Environ Manage* **236**, 413–419.

15. Wu H, Yan HY, Quan Y, Zhao HZ, Jiang NZ, Yin CR (2018) Recent progress and perspectives in biotrickling filters for VOCs and odorous gases treatment. *J Environ Manage* **222**, 409–419.

16. Wang XK, Wang JG, Guo PQ, Guo WL, Li GL (2008) Chemical effect of swirling jet-induced cavitation: degradation of rhodamine B in aqueous solution. *Ultrason Sonochem* **15**, 357–363.

17. Wang XK, Zhang Y (2009) Degradation of alachlor in aqueous solution by using hydrodynamic cavitation. *J Hazard Mater* **161**, 202–207.

18. Liu SX (2019) Experimental study on micro-nano bubble treatment ink wastewater. *Water Technol* **13**, 25–27.

19. Xia ZR, Hu LM (2018) Treatment of organics contaminated wastewater by ozone micro-nano bubbles. *Water* **11**, 55.

20. Khan P, Zhu WJ, Huang F, Gao WL, Khan NA (2020) Micro-nano bubble technology and water-related application. *Water Supply* **20**, 2021–2035.

21. Shi HB, Liu QX, Nikrityuk P (2020) Numerical study of mixing of cavitating flows in a venturi tube. *Can J Chemeng* **99**, 813–828.

22. Chahine GL, Kapahi A, Choi JK, Hsiao CT (2016) Modeling of surface cleaning by cavitation bubble dynamics and collapse. *Ultrason Sonochem* **29**, 528–549.

23. Ge Q, Li XH, Lu YY, Tang Y (2007) Mechanism of organic wastewater treatment by cavitating jets. *J Chongqing Univ (Nat Sci Edn)* **30**, 19–22.

24. Zhu RY, Mao YB, Jiang LY, Chen JM (2015) Performance of chlorobenzene removal in a nonthermal plasma catalysis reactor and evaluation of its byproducts. *Chem Eng J* **279**, 463–471.

25. Mustafa MF, Fu XD, Lu WJ, Liu YJ, Abbas Y, Wang HT, Arslan MT (2018) Application of non-thermal plasma technology on fugitive methane destruction: configuration and optimization of double dielectric barrier discharge reactor. *J Cleaner Prod* **174**, 670–677.

26. Kikuchi K, Takeda H, Rabolt B, Okaya T, Ogumi Z, Saihara Y, Noguchi H (2001) Hydrogen particles and supersaturation in alkaline water from an alkali-ion-water electrolyzer. *J Electroanal Chem* **506**, 22–27.

27. Gogate PR, Pandit AB (2000) Engineering design methods for cavitation reactors II: Hydrodynamic cavitation. *AIChE J* **46**, 1641–1649.

28. Pandit AV, Sarvothaman VP, Ranade VV (2021) Estimation of chemical and physical effects of cavitation by analysis of cavitating single bubble dynamics. *Ultrason Sonochem* **77**, 105677.

29. Attard P (2013) The stability of nanobubbles. *Eur Phys J Spec Top* **223**, 893–914.

30. Sun L, Zhang F, Yang W (2021) Research progress of hydroxyl radicals formed by micro-nano bubble. *Water Purif Technol* **40**, 37–41.

31. Zheng CH, Zhu XB, Gao X, Liu L, Chang QY, Luo ZY, Cen K (2014) Experimental study of acetone removal by packed-bed dielectric barrier discharge reactor. *J Ind Eng Chem* **20**, 2761–2768.

32. Kaori T, Masayuki M, Yusuke N, Jyunko N, Takashi H, Zhao ZW, Yukihiro Y, Shousuke W, et al (2014) ESR measurement of hydroxyl radicals in micro-nano bubble water. *Chem Lett* **43**, 1907–1908.

33. Carpenter J, Badve M, Rajoriya S, George S, Saharan VK, Pandit AB (2017) Hydrodynamic cavitation: an emerging technology for the intensification of various chemical and physical processes in a chemical process industry. *Rev Chem Eng* **33**, 433–468.

34. Takahashi M, Chiba K, Li P (2007) Free-radical generation from collapsing microbubbles in the absence of a dynamic stimulus. *J Phys Chem B* **111**, 1343–1347.

35. Raillard C, Héquet V, Le-Cloirec P, Legrand J (2006) Photocatalytic oxidation of methyl ethyl ketone over sol-gel and commercial TiO_2 for the improvement of indoor air. *Water Sci Technol* **53**, 107–115.